Food Biophysics (2026) 21:25
https://doi.org/10.1007/s11483-026-10116-w

RESEARCH

Encapsulation in Polyvinylpyrrolidone Protects the Ora-Pro-Nobis (*Pereskia Aculeata* Miller) Extracts against the Deleterious effects of *In Vitro* Gastrointestinal Digestion

Valéria Maria Costa Teixeira[1] · Anielle de Oliveira[2] · José Rivaldo dos Santos Filho[1] · Amarilis Santos de Carvalho[2] · Ashley Uchoa[3] · Ana Paula Peron[2] · Filipa Mandim[4] · Eliana Pereira[4] · Fernanda Vitoria Leimann[2] · Alex Graça Contato[5] · Rosane Marina Peralta[1]

Received: 19 October 2025 / Accepted: 13 February 2026

Abstract

Pereskia aculeata Miller, commonly known as ora-pro-nobis, is a South American plant widely found in Brazil and classified as a wild plant. Its leaves are rich in bioactive compounds with reported antioxidant, antimicrobial, and anti-inflammatory properties, supporting growing interest in their use as functional ingredients. This study compared conventional hydroethanolic extraction of antioxidant compounds from *P. aculeata* leaves with a process combining extraction and simultaneous encapsulation, aiming to evaluate differences in stability and bioaccessibility during simulated gastrointestinal digestion. Free and encapsulated extracts (80:20 ethanol: water, v/v) were characterized by Fourier-transform infrared spectroscopy (FTIR), while encapsulated systems were further analyzed by dynamic light scattering (DLS), atomic force microscopy (AFM), and transmission electron microscopy (TEM). Thermal behavior and antiproliferative activity were also evaluated. Total phenolics, flavonoids and antioxidant activity were determined before and after *in vitro* digestion. Extraction and encapsulation yields were 17.25% and 92.75%, respectively, with the encapsulated extract corresponding to 62% of the free extract. Simulated digestion reduced phenolic content, flavonoid levels, and antioxidant activity in both systems; however, significantly lower losses were observed for the encapsulated extract, indicating improved stability. The apparent divergence between better radical-scavenging stability (ABTS/DPPH) and lower TPC/TFC bioaccessibility in the encapsulated samples likely reflects release- and assay-specific effects. PVP can establish hydrogen-bond and dipolar interactions with phenolics, which may slow their diffusion or release and reduce their immediate availability to react with the Folin-Ciocalteu and aluminum-chloride reagents, lowering measured TPC/TFC in the digesta fraction. In contrast, encapsulation can limit oxidative degradation during digestion, thereby preserving redox-active constituents and sustaining radical-scavenging capacity in ABTS/DPPH assays.

Keywords Antioxidant activity · Bioaccessibility · Encapsulation · Gastrointestinal digestion · Ora pro-nobis

Introduction

The genus *Pereskia* includes 17 species that occur only in arid or semi-arid regions native to the Americas [1, 2]. In Brazil, two species *(Pereskia aculeata* Miller *and Pereskia grandifolia*) are native to the Atlantic Forest [3]. Specimens of *P. aculeata* have yellow flowers and ripe yellow fruits, while *P. grandifolia* has purple flowers and ripe purple fruits [4].

P. aculeata, popularly known as ora-pro-nobis, is classified as a wild food plant, a food category recognized

✉ Alex Graça Contato
alexgraca.contato@gmail.com

[1] Postgraduate Program of Biochemistry (PBQ), State University of Maringá (UEM), Maringá, PR, Brazil

[2] Postgraduate Program in Food Technology (PPGTA), Federal Technological University of Paraná (UTFPR), Campo Mourão, PR, Brazil

[3] Undergraduate in Chemical Engineering, Federal Technological University of Paraná (UTFPR), Campo Mourão, PR, Brazil

[4] CIMO, LA SusTEC, Instituto Politécnico de Bragança, Campus de Santa Apolónia, Bragança 5300-253, Portugal

[5] Department of Biochemistry, Chemistry Institute (IQ), Federal University of Rio de Janeiro (UFRJ), Rio de Janeiro, RJ, Brazil

Published online: 09 March 2026

as an important complementary source to combat nutritional deficiencies [5]. The leaves of *P. aculeata* can be used in the preparation of salads, soups, omelets, and pies, and the leaf flour can serve as an enriching ingredient in the formulation of bread, cakes, and pasta. Its leaves are a source of proteins (26% w/w) and also contain significant amounts of minerals, dietary fiber, vitamins A and C, as well as folic acid, trace elements, β-carotene, and ascorbic acid [6–8]. The consumption of *P. aculeata* leaves has been mainly associated with the prevention of iron deficiency, anemia, osteoporosis, cancer, and constipation [9]. Additionally, simple carbohydrates (arabinose, galactose, rhamnose, and glucose) and polysaccharides (arabinogalactan and galactomannan) have already been identified in the leaves of *P. grandifolia* and *P. aculeata*. These biopolymers can chelate several ions, including Fe^{2+}, Co^{2+}, and Ni^{2+} [10].

Phenolic compounds have been shown to be safe and effective as nutraceutical agents in food formulations [11–14]. However, their applications may be limited by its low bioavailability, unpleasant taste, low stability, and high sensitivity to oxidative factors [15]. In recent years, the fruits and leaves of ora-pro-nobis have been the subject of studies aimed at evaluating their composition in phenolic compounds. Several phenolic compounds have been identified in ora-pro-nobis leaf extracts including hordenine, di-tert-butylphenol, petunidin, quercetin, cis-caffeic acid, trans-caffeic acid, caffeic acid, rutin, isorhamnetin, kaempferol, chicoric acid, caffeoyl-hexaric acid, coumaroyl-hexaric acid, and glycosylated derivatives of these compounds [16–19]. However, a recent study with extracts from *ora-pro-nobis* leaves and fruits demonstrated a marked reduction in phenolic content and antioxidant capacity following simulated gastrointestinal digestion [19]. This loss of bioactivity highlights the susceptibility of these compounds to degradation under digestive conditions. Encapsulation has emerged as a promising strategy to mitigate such losses, protecting bioactive molecules from adverse pH, enzymatic, and oxidative environments, while potentially enhancing their stability and bioavailability. One effective approach involves the use of synthetic polymers, such as polyvinylpyrrolidone (PVP), a water-soluble and hydrophilic macromolecule known for its capacity to form protective matrices around sensitive compounds [20, 21].

From a regulatory and application standpoint, polyvinylpyrrolidone is authorized as a food additive in several jurisdictions (e.g., PVP as E 1201 in the EU and permitted uses described in 21 CFR 173.55 in the USA). In the present work, PVP was used at 0.5% (w/v) in the extraction/encapsulation medium (5 mg/mL), a level compatible with polymer-to-extract ratios commonly explored in solid-dispersion micro/nanoencapsulation for functional ingredients. Nevertheless, the permitted use level depends on the specific food category and local legislation, and future product development should confirm regulatory compliance with the intended application, as well as sensory and labeling constraints. Polysorbate 80 (Tween 80; E 433; 21 CFR 172.840) was included at 0.05% (w/v) as a food-grade non-ionic surfactant to improve wetting and dispersion during high-shear processing and to reduce particle aggregation during formation and redispersion.

Encapsulation of *ora-pro-nobis* (*Pereskia aculeata*) plant extracts in PVP represents a promising strategy to preserve and control the release of their bioactive compounds during gastrointestinal digestion. PVP is a biocompatible and water-soluble polymer widely recognized for its ability to form protective matrices around sensitive molecules, shielding them from adverse environmental conditions such as temperature variations, pH changes, and enzymatic degradation. Different works have studied the stability of PVP encapsulated extracts. Additionally, studies of Rehman et al. and Han et al. pointed out that PVP exhibited the highest stability among all tested surfactants, outperforming others in terms of zeta potential [22, 23]. By encapsulating ora-pro-nobis extracts in PVP, at least in theory, bioactive constituents, such as polysaccharides, proteins, and antioxidant compounds, can be protected from premature degradation, thereby retaining their structural integrity and functional properties in accordance with the results obtained from previous studies with other extracts and pure compounds [24, 25]. This approach not only could enhance the stability and efficacy of *ora-pro-nobis* bioactives but also increases their potential applications in functional foods, nutraceuticals, and therapeutic formulations, contributing to improved health benefits and product shelf life. Given the several uses of ora-pro-nobis leaves listed above, this study aimed at comparing simple extracts of *P. aculeata* leaves with encapsulated ones in terms of their stability during simulated gastrointestinal digestion.

Materials and Methods

Materials

Flour of *Pereskia aculeata* (ora-pro-nobis) dried leaves, of organic quality, was purchased from Flora Bioativas (Joinville, SC, Brazil) (−27.18697918436603, −48.687579803019105). The following reagents were obtained from Sigma Chemical Co. (St. Louis, MO, USA): polyvinylpyrrolidone (PVP, 40,000 g/mol), 2,2-diphenyl-1-picrylhydrazyl (DPPH), 2,4,6-Tris(2-pyridyl)-s-triazine (TPTZ), and 2,2'-azino-bis (3-ethylbenzothiazoline-6-sulfonic acid) diammonium salt (ABTS), porcine pancreatic α-amylase (Type VI-B, 10 units/mg solid). All remaining

reagents used in antioxidant, digestion, and cytotoxicity assays are detailed in the respective subsections.

Extraction and Simultaneous Extraction/ Encapsulation

For the extraction and encapsulation of bioactive compounds from ora-pro-nobis, the methodology was adapted from previously published articles [26, 27]. A mixture of ethanol: water in an 80:20 (v: v) ratio was used as the solvent. For the extraction, 17.5 g of ora-pro-nobis leaf flour were added to 200 mL of the ethanol: water solution, followed by agitation using an Ultra-Turrax (IKA, T25, Staufen, Germany) at 12,000 rpm for 15 min, with an ice bath to maintain the temperature and prevent overheating. For the extraction, 17.5 g of ora-pro-nobis leaf flour were added to 200 mL of the ethanol: water solution, followed by agitation using an Ultra-Turrax (IKA, T25, Staufen, Germany) at 12,000 rpm for 15 min, with an ice bath to maintain the temperature and prevent overheating. Although higher solid-to-liquid ratios are often recommended, this ratio was selected based on preliminary optimization to ensure efficient homogenization under high-shear conditions and compatibility with the simultaneous extraction/encapsulation process. The mixture was then filtered using a vacuum pump (Prismatec, Sao Paulo, Brazil) and dried in an air circulation oven (Cienlab, Santa Catarina, Brazil) at 50 °C for 24 h.

For the simultaneous extraction/encapsulation process, the ora-pro-nobis leaf flour (17.5 g), the ethanol: water solution (200 mL), PVP (0.5% w/v), and Tween 80 (0.05% w/v) were mixed and subjected to agitation in the Ultra-Turrax under the same conditions used to obtain the pure extract. Subsequently, the encapsulated extracts were dried in an oven (50 °C–24 h). After drying, both the free extract and the encapsulated extract were stored in a freezer until use. The extraction and encapsulation yields were calculated according to Eq. (1), in which MI stands for the initial solid content before drying and MF the final solid content (after drying):

PVP (0.5% w/v) was selected as a hydrophilic, film-forming carrier to promote solid dispersion and protect labile bioactives, while Tween 80 (0.05% w/v) was used as a low-level non-ionic surfactant to facilitate wetting, improve dispersion under Ultra-Turrax shear, and minimize aggregation during particle formation and redispersion.

$$R_{ext}(\%) = \left(\frac{M_F}{M_I}\right) \times 100 \quad (1)$$

The encapsulation yield (R_{ENC}, in percentage) was calculated based on the content remaining after drying (M_F), considering that extraction and encapsulation occurred in a single step, the recovered mass (M_{opn}), the mass of PVP (M_{pvp}), and the mass of Tween 80 (M_{tween}), according to Eq. (2):

$$R_{ENC} = \left(\frac{M_F}{M_{opn} + M_{pvp} + M_{tween}}\right) \times 100 \quad (2)$$

The mass of extract (M_{ext}) present in the encapsulated formulation was calculated according to Eq. (3):

$$M_{ext} = \left(\frac{M_{opn}}{M_F}\right) \times R_{ENC} \quad (3)$$

Characterization of Extracts and Particles

Fourier Transform Infrared Spectroscopy (FTIR)

The characterization of ora-pro-nobis extracts was done using FTIR (Fourier transform infrared spectroscopy) on a Shimadzu IR Affinity-1 instrument (Kyoto, Japan) at the Federal University of Technology – Paraná, Campo Mourão Campus, Paraná (UTFPR). The free and encapsulated extracts before and after *in vitro* digestion, the physical mixture and PVP were dispersed in potassium bromide (KBr) and pelletized using a pellet press and a hydraulic press. FTIR spectra were obtained in transmission mode in the wavenumber range of 400 to 4,000 cm^{-1}, with 32 scans and a resolution of 4 cm^{-1}. Peak positions were identified by visual inspection of spectra, and functional-group assignments were performed based on literature reports for PVP and plant-derived matrices (no automated peak-assignment software was used).

Dynamic Light Scattering (DLS)

Dynamic light scattering (DLS) was used to determine the size distribution, polydispersity index (PDI), mean size (Dz), and zeta potential of the particles using a Litesizer 500 (Anton Paar, Sao Paulo, Brazil). Samples were dispersed in ultrapure water at 1.0 mg/mL and gently homogenized; when needed, further dilution was applied to avoid multiple scattering. Measurements were performed at 25 °C in triplicate using independently prepared dispersions, and results are reported as mean ± SD.

Atomic Force Microscopy (AFM)

For atomic force microscopy (AFM), the ora-pro-nobis particles were diluted to 1.0 mg/mL in ultrapure water (Milli Q). Thereafter, 50 µL of the sample were added to a previously cleaned mica V-1 substrate (Electron Microscopy Science,

USA). The samples were dried in an oven at 30 °C for 3 h before analysis. Images were obtained using an atomic force microscope (Agilent® SPM 5500, USA) in intermittent contact mode (tapping), using the NSC35 cantilever (µmasch®, Estonia) with a force constant of 7.5 N/m and a frequency of 190 kHz. Three distinct regions (A, B, and C) were scanned with areas of 8·8, 4·4, 2·2, and 1·1 µm, at a scan rate of 1.44 ln/s and a resolution of 512 p. Image processing was performed using the Gwyddion software (v 2.50). At least three independent sample preparations were analyzed, and representative images are shown.

Transmission Electron Microscopy (TEM)

The morphology of the synthesized particles was analyzed by transmission electron microscopy (TEM) (JEOL-JEM 1400, Tokyo, Japan), with a drop of encapsulated extract before and after *in vitro* digestion, dried and resuspended (1 mg/mL) in distilled water, placed on a copper grid coated with a 300-mesh carbon film. The grid was then placed in a desiccator, where it remained for 24 h before being analyzed.

Thermogravimetric Analysis (TGA) and differential Scanning Calorimetric (DSC)

Thermogravimetric analyses (TGA) were conducted in a nitrogen atmosphere, with temperatures ranging from 0 to 600 °C, at a heating rate of 10 °C·min^{-1}, using a Netzsch instrument, model STA 409 PG (Burlington, MA, USA). The differential scanning calorimetry (DSC) analysis of the samples was performed using a thermal analyzer (TA Instruments, model DSC Q20, Waters, Milford, MA, USA). The samples were heated to 250 °C with a heating rate of 10 °C/min^{-1} in a nitrogen atmosphere (50 mL/min).

Antiproliferative and Hepatotoxic Activity

The ora-pro-nobis extract's capacity to inhibit cell proliferation was assessed using the colorimetric sulforhodamine B (SRB) assay, according to the methodology of Barros et al. [28]. The following tumor cell lines were used: AGS (gastric adenocarcinoma), Caco-2 (colorectal adenocarcinoma), MCF-7 (breast carcinoma), and NCI-H460 (lung carcinoma). All these tumor cell lines were commercially obtained from the Leibniz Institute DSMZ - German Collection of Microorganisms and Cell Cultures GmbH (Braunschweig, Germany). The tumor cell lines were following the manufacturer's guidelines. Besides tumor cells, extracts hepatotoxicity was also tested using a primary culture obtained from pig liver (PLP2) and established in the laboratory following the procedure previously described [29].

The extract was re-dissolved in water at a final concentration of 8 mg/mL, from which different concentrations were obtained to be tested (between 8 and 0.125 mg/mL). Each extract concentration (10 µL) was incubated with the tested cell lines suspensions (1×10^4; 190 µL) in 96-well microplates for 72 h (final concentrations tested between 400 and 6.25 µg/mL). The microplates were incubated at 37 °C in a humidified atmosphere with 5% CO_2. After the incubation period, cold trichloroacetic acid (TCA, 10% w/v) was added to each well and incubated for 60 min at 4°C. The microplates were washed with deionized water and dried. Then, a sulforhodamine B (SRB, 0.057% w/v) solution was added, and the plate was incubated for 30 min at room temperature. The plate was then washed with acetic acid (1% v/v) to remove excess SRB and left to dry in air. The SRB was solubilized with TRIS buffer (10 mM, pH 7.4) using a microplate shaker (Stat Fax-2100). Absorbance was measured at 540 nm using a microplate reader (Bio-Tek Instruments, ELX800, Inc., Winooski, VT, USA), with ellipticine as the positive control. Data were normalized to the untreated control group (considered as 100% viability), and results were expressed as GI_{50} values in µg/mL.

Cytotoxicity Test in Allium Cepa Root Meristems

Obtaining and Rooting the Bulbs

Bulbs of *Allium cepa* (onion) were purchased from an organic garden. Before starting the experiments, bulbs were scarified to remove dry cataphylls and washed in distilled water. Soon afterwards, bulbs were placed in contact with their respective treatments where they remained for rooting for 5 days (120 h). Five replications of bulbs were used for both control and tests. Analyses were performed for cytotoxicity and genotoxicity. Distilled water was used as a control.

Assessments of phytotoxicity, Cytotoxicity and Genotoxicity

Toxicity evaluation in *A. cepa* bulb roots was performed according to Fiskesjö [30] with the modifications introduced by Filipi et al. [31]. For evaluation of the cytotoxic and genotoxic potentials, roots were collected from each bulb and fixed in Carnoy 3:1 (methanol: acetic acid) for up to 24 h. Then, roots were hydrolyzed in 1 N HCl. After staining, meristematic regions were separated and mounted on slides using the crushing technique. An optical microscope at 400· magnification was used to analyze the slides. The cytotoxic potential was determined by the Mitotic Index (MI), which was calculated according to Eq. (4). The *Allium* cepa assay is widely used as a low-cost, sensitive bioindicator to screen cytotoxic and genotoxic effects of complex

mixtures, supporting a first-tier safety assessment of botanical extracts intended for food-related applications.

$$MI = \left(\frac{\text{Total EquationNumber of dividing cells}}{\text{Total EquationNumber of cells analyzed}} \right) \times 100 \quad (4)$$

Cells in interphase and cells in prophase, metaphase, anaphase, and telophase were counted. From each bulb, 2000 cells were counted, totaling 10,000 cells analyzed per treatment.

The genotoxic potential was determined by the Index of cellular changes (ICC), established by the number of cellular changes observed in root meristems after exposure to treatments (Eq. (5)):

$$ICC = \left(\frac{\text{Number of cell changes}}{1000} \right) \times 100 \quad (5)$$

A total of 200 cells per bulb were analyzed, totaling 1,000 cells per treatment. The following cellular alterations were considered: micronuclei, viscosity, chromosomal abnormalities in prophase, metaphase, anaphase and telophase, chromosomal breaks, chromosomal bridges in anaphase and telophase, multipolar spindles and polyploidy.

In Vitro Digestion of Hydroalcoholic Extracts and Encapsulated Hydroalcoholic Extracts

To evaluate a potential protective effect of the encapsulation of ora-pro-nobis leaf extracts, the simulated *in vitro* gastrointestinal digestion of hydroalcoholic extracts and encapsulated hydroalcoholic extracts was performed following the INFOGEST protocol [32]. A concise table summarizing the latest INFOGEST static *in vitro* digestion protocol with pH, duration, and main enzyme is presented in Table 1. At the end of the process, the materials were lyophilized and stored at −20 °C until use.

Total Phenolic and Flavonoid Content

The total phenolic content was determined by the Folin-Ciocalteu method [33]. The test tubes with the samples and reagent were protected from light and kept at room temperature for 1 h. Absorbance was measured at the wavelength of 725 nm using a UV-VIS spectrophotometer (Red Tide, model UV USB650, Ocean Optics, Orlando, FL, USA). A standard curve was previously prepared using different concentrations of gallic acid (2 to 16 µg/mL; y = 0.0472x – 0.0324, R^2 = 0.9963). The total phenolic content was expressed in micrograms of gallic acid equivalent per milligram of sample ($\mu gGA/mg_{sample}$).

The total flavonoid content was determined following the protocol of Alothman et al. [34]. Briefly, sample, distilled water, and 5% (w/v) $NaNO_2$ were added to the tubes. After 5 min, 10% $AlCl_3$ was added, and after 6 min, 1 M NaOH was added. The mixture was vortexed and immediately subjected to absorbance reading at 510 nm. A calibration curve was prepared using a standard catechin solution (10, 20, 40, 60, 80, and 100 mg/L; y = 0.004x – 0.0003; R^2 = 0.9997). The results were referred to the fresh weight and expressed as µg of catechin equivalents per gram of sample ($\mu gCEQ/g_{sample}$).

The bioaccessibility of the total phenolic content and the total flavonoid content was calculated according to Eq. (6):

$$Bioaccessibility(\%) = \left(\frac{Digested\ sample}{\text{Non-digested sample}} \right) \times 100 \quad (6)$$

Evaluation of Antioxidant Activity

The antioxidant capacity of the free and encapsulated extracts, with or without simulated digestion, was evaluated using four different methods: DPPH, ABTS, FRAP, and TBARS. The determination of antioxidant capacity by the DPPH method (2,2-diphenyl-1-picrylhydrazyl) as a free radical followed the methodology described by Thaipong et al. [35] with some modifications. Absorbance was measured at 515 nm using a UV-VIS spectrophotometer (Red Tide, model UV USB650, Ocean Optics). The values were calculated according to Eq. (7), expressed as IC_{50}, which is the concentration required to inhibit or decolorize 50% of the evaluated activity.

$$\text{DPPH decolorization } (\%) = \left(\frac{A_{control} - A_{sample}}{A_{control}} \right) \times 100 \quad (7)$$

Evaluation of the antioxidant capacity by the ABTS method (2,2'-azinobis (3-ethylbenzothiazoline-6-sulfonic)) followed the method of Thaipong et al. [35] with some modifications. The working solution was prepared by mixing equal volumes of an ABTS solution at 7.4 mmol/L and a potassium persulfate solution at 2.6 mmol/L, which was left to react in the absence of light for 12 h. Absorbance (A) of the samples was measured at 734 nm (Red Tide spectrophotometer, model UV USB650, Ocean Optics). The percentage decolorization was calculated according to Eq. (8):

Table 1 Main conditions of the INFOGEST *in vitro* digestion protocol [32]

Phase	pH	Duration	Main enzyme (final activity)
Oral	7.0	2 min	Salivary amylase (~75 U/mL)
Gastric	3.0	2 h	Pepsin (~2,000 U/mL)
Intestinal	7.0	2 h	Pancreatin (trypsin ~ 100 U/mL, lipase ~ 60 U/mL) + bile salts (10 mM)

$$\text{ABTS decolorization } (\%) = \left(\frac{A_{control} - A_{sample}}{A_{control}}\right) \times 100 \quad (8)$$

For evaluating the potential capacity of the extracts as inhibitors of lipid peroxidation the method of the thiobarbituric acid reactive substances (TBARS) was used. The protocol described by Corrêa et al. [36] and Reis et al. [37] was followed. The rat brains were dehydrated and homogenized in cold Tris-HCl buffer (20 mM, pH 7.4). The samples were incubated with $FeSO_4$ (10 mM) and ascorbic acid (0.1 mM) at 37 °C for 1 h, followed by the addition of trichloroacetic acid (28% w/v) and thiobarbituric acid (TBA, 2% w/v), and the mixture was heated at 80 °C for 20 min. After centrifugation at 7,000*g* for 15 min to remove the precipitated protein, the intensity of the color of the malondialdehyde-thiobarbituric acid (MDA-TBA) complex in the supernatant was measured as its absorbance at 532 nm. The percent decolorization was calculated using Eq. (9):

$$\text{TBARS decolorization } (\%) = \left(\frac{A_{control} - A_{sample}}{A_{control}}\right) \times 100 \quad (9)$$

The percentage decolorization values of DPPH, ABTS and TBARS obtained by means of Eqs. (7)-(9) as a function of the extract concentrations were used for determining the IC_{50} values by numerical interpolation, expressed as µg/mL.

The FRAP (ferric reducing antioxidant power) assay was performed following the methodology of de Contato et al. [38] using the FRAP reagent (10 mM TPTZ in 40 mM HCl, 20 mM ferric chloride, and 300 mM acetate buffer, pH 3.6, in a v/v/v ratio of 1:1:10). The tubes were protected from light and placed in a water bath at 37 °C for 30 min. After this period, absorbance was measured at 595 nm (Ocean Optics, Red Tide USB650 Optical Fiber Spectrometer, USA). A Trolox standard curve was used for quantification ($y = -0.0012x + 0.0039$, $R^2 = 0.999$). The results were expressed as micromoles of Trolox equivalent per gram of sample ($\mu MTE/g_{sample}$).

Statistical Analysis

For quantitative assays, data distribution was assessed for normality (Shapiro–Wilk test) and homoscedasticity (Levene's test). When assumptions were met, results were compared using analysis of variance (ANOVA) and Tukey's post hoc test with a significance level of 5% ($p < 0.05$) using Matlab R2024a software (MathWorks). The IC_{50} calculation was performed using GraphPad Prism software with nonlinear regression. For the cytotoxicity analysis of *Allium cepa*, the data were tested for normality by the Lilliefors test and were considered non-normal. Kruskal–Wallis analysis of variance followed by Dunn's post hoc test ($p \leq 0.05$) was applied to analyze phytotoxicity, cytotoxicity, and genotoxicity data, using the RStudio software.

Results and Discussion

Characterization of the Free and Encapsulated Extract

Extraction and Encapsulation Yields

The extraction yield of ora-pro-nobis free extract was 17.25% (Eq. 1). The yield obtained during encapsulation was the same, as the encapsulation process did not alter the extraction efficiency. The encapsulation yield was 92.75% (Eq. 2). Considering the composition of the encapsulated formulation — ora-pro-nobis extract, polyvinylpyrrolidone (PVP) as encapsulating agent, and Tween 80 as surfactant — it was estimated that the extract represented approximately 62% of the total mass of the encapsulated product obtained by the solid dispersion technique (Eq. 3).

FTIR Spectroscopy Analyses

Fourier Transform Infrared (FTIR) spectroscopy was performed on free and encapsulated extracts, both before and after simulated digestion, as well as on PVP and on a physical mixture of free extract and PVP (Fig. 1A-D).

All samples except PVP exhibited a broad band in the 3305–3340 cm^{-1} range, characteristic of hydroxyl (O–H) groups. These groups are commonly found in plant-derived compounds such as polysaccharides and phenols, which are associated with antioxidant properties and strong hydrogen bonding with water [39, 40]. Peaks corresponding to aliphatic C–H stretching were observed in the encapsulated extract (2924 cm^{-1}) and the physical mixture (2928 cm^{-1}), while the digested free extract showed a peak at 2934 cm^{-1}. Similar bands for *ora-pro-nobis* have been reported at 2930 cm^{-1} [41] and 2924 cm^{-1} [42]. Bands in the carbonyl stretching region showed variations between samples. The free extracts presented peaks at 1605 cm^{-1} (digested) and 1617 cm^{-1} (undigested), while the encapsulated extracts exhibited peaks at 1647 cm^{-1} and 1650 cm^{-1}. PVP displayed a peak at 1656 cm^{-1}, and the physical mixture at 1640 cm^{-1}. This region corresponds to C=O stretching in carboxyl groups and C=C stretching [39, 40], and may also reflect primary and secondary amide vibrations from mucilage proteins present in *ora-pro-nobis* leaves [43]. Comparable bands have been observed at 1613 cm^{-1} [44]. A band at 1440 cm^{-1} in the encapsulated extracts is associated with C–H vibrations in CH_3/CH_2 groups and aromatic compounds, including flavonoids [44, 45]. Symmetric

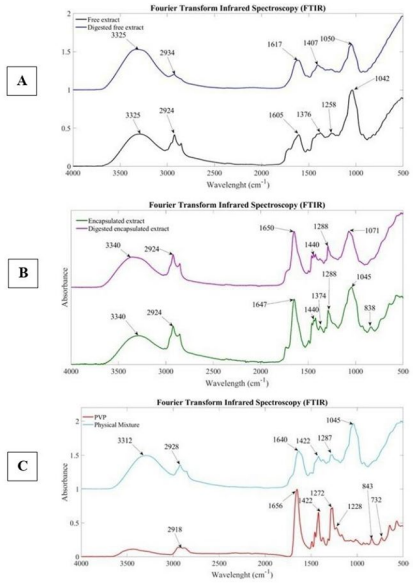

D Characteristic FTIR bands of PVP, physical mixture, and free and encapsulated extracts of ora-pro-nobis.

Wavelength (cm ^{1})	Function group
3600 – 3200	O-H
2960 – 2850	C-II Aliphatic
1605-1656	C=C
1400-1407	C-H
1420	COO
1440	C-H
1258-1288	C-O
1228	CH_2
1376-1374	CH_3

Fig. 1 FTIR spectra of free and PVP-encapsulated *ora-pro-nobis* extracts and related samples obtained in the wavenumber range of 4000–400 cm^{-1}. (**A**) Spectra of the undigested free extract and digested free extract. (**B**) Spectra of the undigested PVP-encapsulated extract and digested encapsulated extract. (**C**) Spectra of the encapsulating agent (PVP) and the physical mixture containing 62% free extract and 38% PVP. (**D**) Characteristic FTIR bands of PVP, physical mixture, and free and encapsulated *ora-pro-nobis* extracts

COO^- stretching appeared at 1422 cm^{-1} in PVP, the physical mixture, and encapsulated extracts, in agreement with observations for *ora-pro-nobis* mucilage hydrogels [46].

Characteristic PVP absorptions were evident: strong carbonyl absorption in the 1656–1640 cm^{-1} range and C–N stretching in the N-vinylpyrrolidone ring at 1287–1270 cm^{-1} [41, 45]. The latter was also present in the physical mixture and encapsulated extracts. A scissoring vibration of cyclic CH_2 groups was observed near 1420 cm^{-1}, while a weaker band at 1228 cm^{-1} corresponded to CH_2 twisting in the pyrrole ring [45]. Bands at 1374–1376 cm^{-1}, attributed to amide III (C–N stretching) from oligopeptidic bonds in *ora-pro-nobis* membranes [41], appeared in digested samples. C–H bending in the 1288–1269 cm^{-1} range was detected in encapsulated extracts, the physical mixture, and PVP, suggesting interactions between the extract and encapsulating agent. Amide III bands were found around 1050–1042 cm^{-1} in free extracts and at 1045 cm^{-1} in the undigested encapsulated extract and physical mixture. The digested encapsulated extract showed a shift to 1071 cm^{-1}, which may correspond to C–O stretching in ether linkages [44].

Overall, *in vitro* digestion led to decreased band intensities and slight peak shifts, likely due to pH variations and enzymatic activity under gastric conditions (Table 1).

Dynamic Light Scattering (DLS)

The zeta-potential is a key parameter influencing electrostatic interactions between particles in an aqueous medium [47]. When the zeta-potential value of all suspended particles is highly negative or positive, it induces repulsion and disrupts the electrostatic interaction between each particle [48], phenomena that may result in low stability of the microcapsules. The undigested ora-pro-nobis particle exhibited a lower zeta-potential value when compared to the digested particle (Table 2).

The value of the average particle diameter (Dz) is an indicator of the surface area and activity of the particles in the evaluated system. According to Peanparkdee et al. [48], Dz can influence the bioavailability of phenolic compounds, as this availability depends on the particle size, as well as how the particle components react to acids and enzymatic actions in the digestive tract. No significant differences ($p > 0.05$) were observed between the digested and undigested ora-pro-nobis particles, which may indicate uniformity during the digestive process. Additionally, the particles exhibited a unimodal shape, as they showed only one peak, as shown in Fig. 2, with an average distribution of 0.4 ± 0.1. Gao et al. [49] evaluated the stability of β-lactoglobulin/arabic gum nanoparticle complexes under simulated gastrointestinal conditions and observed no significant differences between the digested and undigested particles.

The zeta potential varies with pH, becoming more positive or more negative under acidic or basic conditions, especially for molecules that contain multiple functional groups, as is the case with the plant matrix. At a low pH range, such as in the gastric phase (pH 2.0), hydroxyl groups can be protonated (gaining or losing an H^+), acquiring a positive charge. However, at a higher pH, such as in the salivary and intestinal phases of digestion (pH 7.5), these sites become

Table 2 Average particle size of PVP and ora-pro-nobis, zeta potential, and polydispersity index before and after *in vitro* digestion

Samples	Average particle size (nm)	Zeta potential (mV)	Polydispersity index (%)
Undigested Particles	479.43 ± 32.27^{a}	−23.86 ± 1.12^{a}	22.63 ± 0.35^{a}
Digested Particles	494.90 ± 30.70^{a}	−36.70 ± 0.45^{b}	26.76 ± 1.84^{a}

DLS/zeta potential values are reported as mean ± SD ($n = 3$). ^{a}There is no significant difference compared with undigested particles; ^{b}There is significant difference compared with undigested particles

negatively charged. This fluctuation in pH values alters the protonation level of functional groups on the particle surface, which in turn changes the zeta potential value [47]. During gastric digestion, it is expected that, due to enzymatic action and pH changes, particles that were initially aggregated will disperse. This is associated with an increase in the magnitude of the zeta potential (from −23 mV to −36 mV), indicating greater electrostatic repulsion between particles, contributing to their disaggregation and thus favoring the exposure of active sites to enzymatic action. Therefore, in the gastric region, greater colloidal instability is expected, associated with a more negative zeta potential, which may enhance the digestion and bioavailability of encapsulated compounds.

The polydispersity index (PDI) is a parameter used to define the particle size distribution, with values ranging from 0 to 1. A value of 0 represents a highly homogeneous material (monodispersed), while a value of 1 indicates a highly heterogeneous material (polydispersed) [50]. Both undigested and digested particles showed highly positive values, indicating a highly polydispersed particle size distribution with 100% intensity (Figs. 2 and 3). This suggests that the particles have a uniform size, indicating pronounced homogeneity, exhibiting a spherical shape and nanometric size (Fig. 3). The shape and size of the particles are related to the solid dispersion technique used in the encapsulation process [51].

Transmission Electron Microscopy (TEM)

Figure 4A-C depict the undigested encapsulated extract samples, while Fig. 4D-F present the corresponding digested samples.

TEM analysis revealed that the undigested particles appeared more aggregated and exhibited a darker contrast (Fig. 4A), whereas the digested particles were more dispersed and displayed a slightly lighter contrast (Fig. 4D). This variation in image contrast likely reflects differences in particle density. The lighter appearance of the digested particles suggests a lower density, possibly due to partial hydrolysis of the PVP matrix and subsequent release of the encapsulated extract, thereby altering the material's overall density. It is known that the electron beam in TEM interacts with the sample, and materials with higher crystallinity and density tend to appear darker [52]. Although PVP is an amorphous polymer, the degradation of its matrix and release of bioactive compounds during digestion could produce similar changes in image contrast. Post-digestion, the particles exhibited a porous morphology (Fig. 4D), which can be attributed to pH fluctuations and enzymatic activity during simulated gastrointestinal conditions. The undigested particles had an average diameter of 153 ± 50 nm, slightly larger than the size estimated by DLS, a discrepancy likely arising from differences in sample preparation, as TEM measures dried particles. The digested particles presented an average

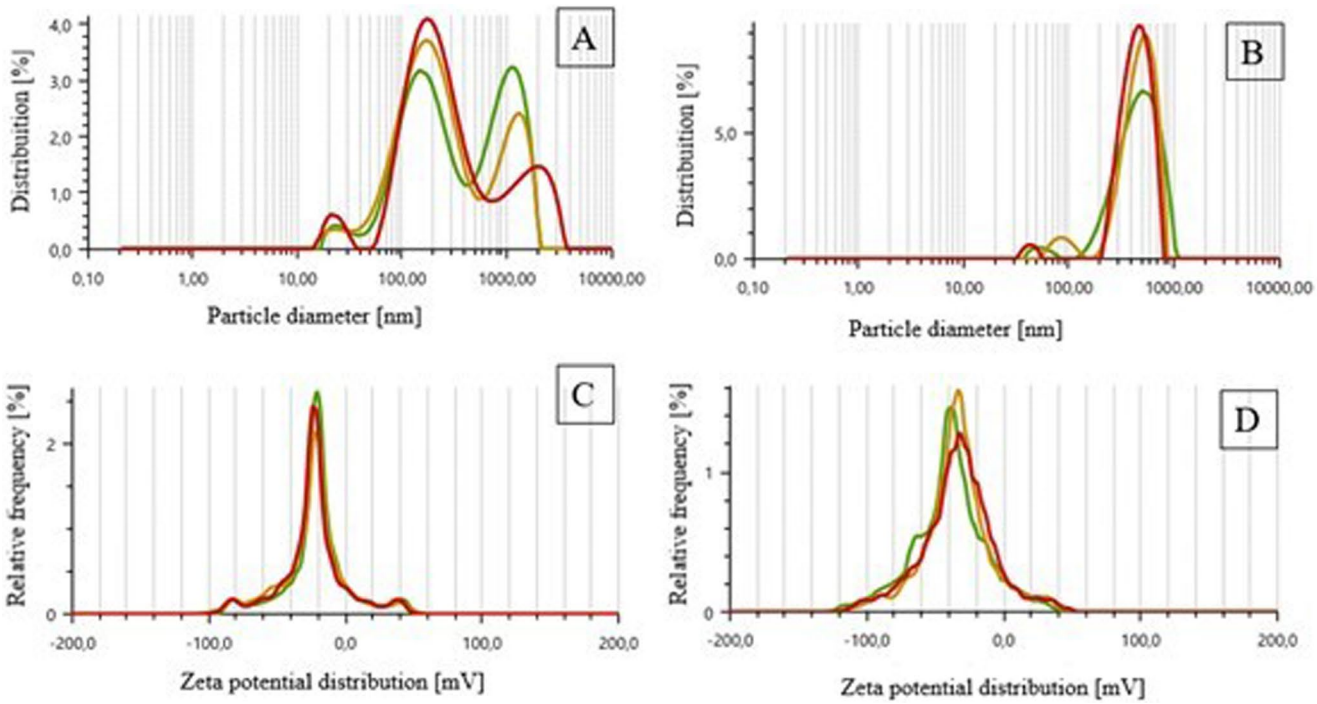

Fig. 2 Average particle diameter of ora-pro-nobis in intensity (nm): (**A**) Undigested particle; (**B**) Digested particle. Zeta potential distribution: (**C**) Undigested particle; (**D**) Digested particle

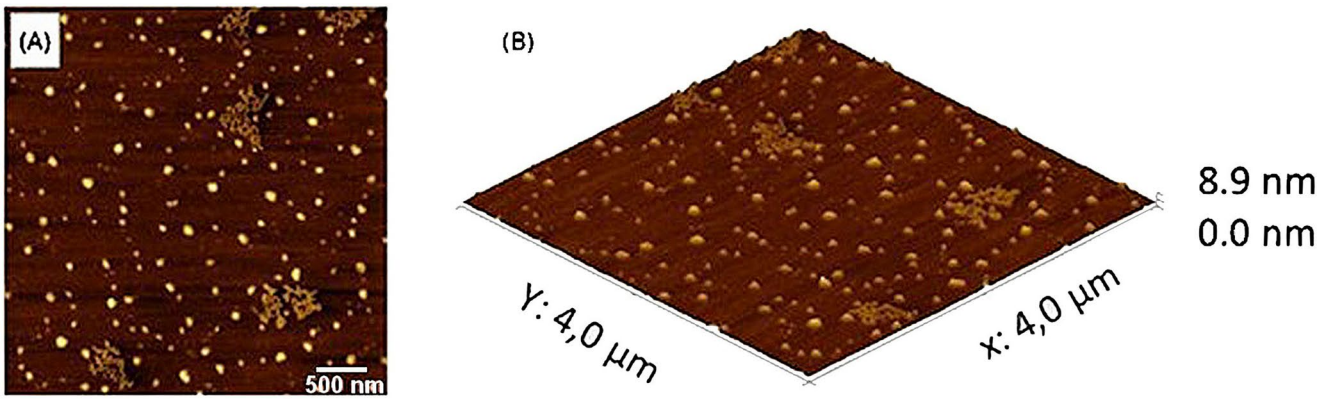

Fig. 3 Atomic force microscopy images of the encapsulated ora-pro-nobis extract at a resolution of 512 p

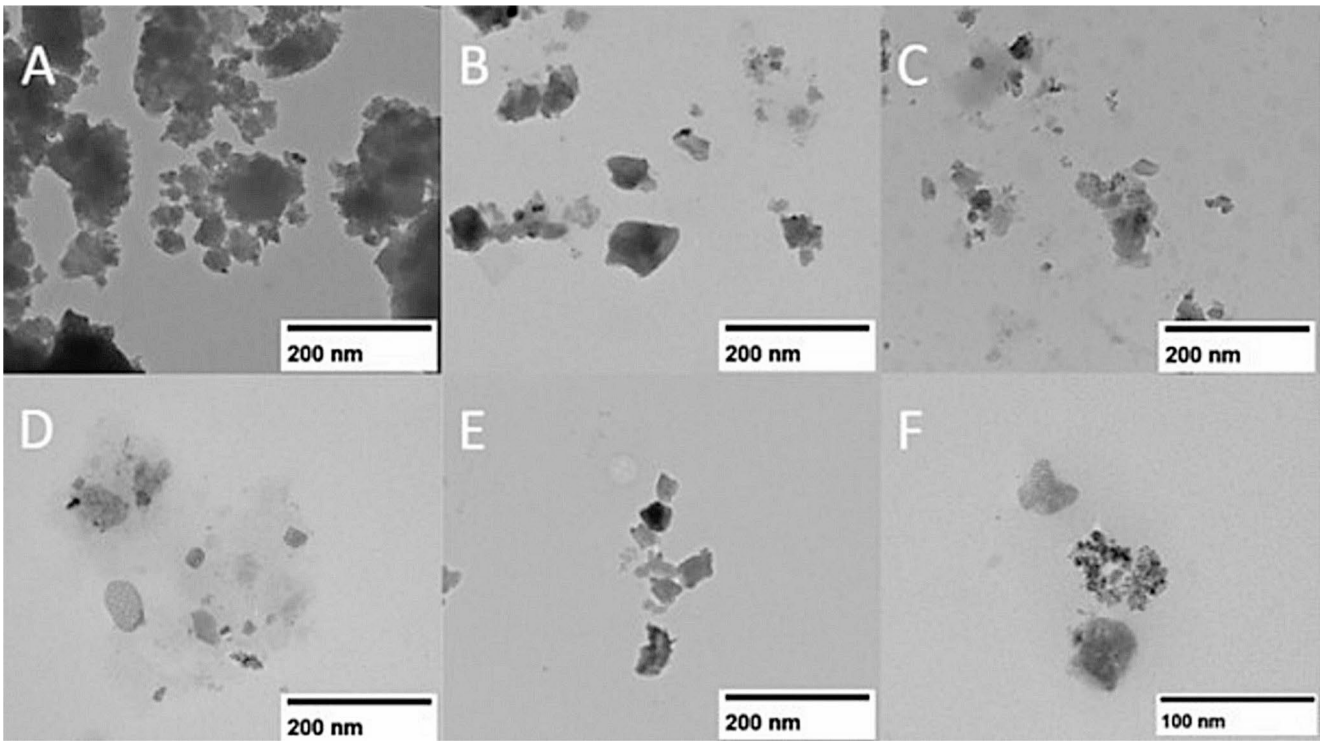

Fig. 4 Characterization of encapsulated extracts by transmission electron microscopy (TEM). (**A**, **B**,and **C**) Encapsulated ora-pro-nobis extracts before simulated gastrointestinal digestion; (**D**, **E**,and **F**) Encapsulated extracts after digestion. Images A, B, C, D, and E are at a scale of 200 nm, and image F is at a scale of 100 nm

diameter of 158 ± 25 nm. Average diameters were obtained by measuring individual particles from TEM micrographs using ImageJ ($n = 50$ particles per condition).

PVP is inherently water-soluble; however, when it interacts with compounds from the plant matrix via solid dispersion, hydrogen bonding can occur. These interactions cause the polymer to contract, producing a water-insoluble network that facilitates nanoparticle formation. In contrast, pure PVP without interaction with another matrix remains soluble and does not form nanoparticles, making TEM analysis of pure PVP impractical.

Thermogravimetric Analysis (TGA) and differential Scanning Calorimetry (DSC)

Thermogravimetric analyses were performed on the free extract, the encapsulated extract (before and after *in vitro* digestion), pure PVP, and a physical mixture consisting of free extract (62%) and PVP (38%) (Fig. 5). PVP exhibited an initial degradation phase between 0 and 70 °C, with a mass loss of approximately 10%, followed by a second stage between 320 and 450 °C, resulting in complete mass loss (Fig. 5A). Similar results were reported by Oliveira

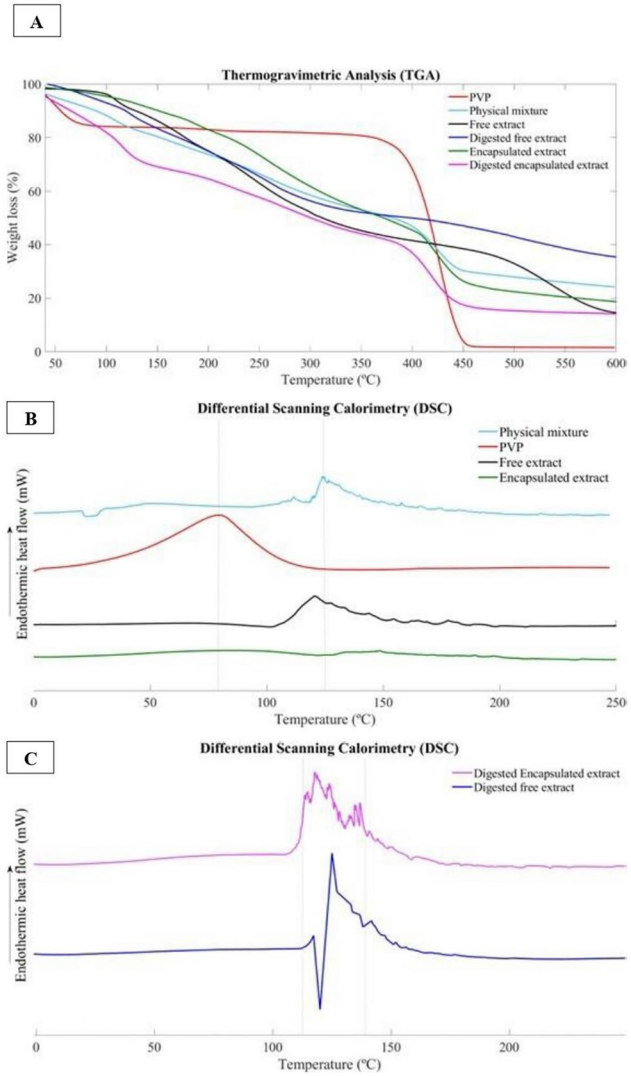

Fig. 5 Thermal analyses of free and PVP-encapsulated extracts, physical mixture, and PVP before and after *in vitro* digestion. (**A**) Thermogravimetric analysis (TGA) of free extract before (blue) and after digestion (black), encapsulated extract before (cyan) and after digestion (magenta), PVP (red), and physical mixture (green). (**B**) Differential scanning calorimetry (DSC) analysis of the physical mixture, PVP, free extract, and encapsulated extract before *in vitro* digestion. (**C**) Differential scanning calorimetry (DSC) analysis of the free extract and encapsulated extract after *in vitro* digestion

et al. [53], who investigated the thermal stability of PVP and extracts encapsulated with this polymer. The physical mixture showed an initial mass loss of 55% up to 400 °C, followed by a second stage between 400 and 450 °C, retaining approximately 35% of its original mass (Fig. 5A). The encapsulated extract prior to *in vitro* digestion did not display an endothermic peak, unlike the other samples, which may be attributed to the protective effect of PVP during encapsulation, enhancing the thermal stability of the ora-pro-nobis extract (Fig. 5B).

The encapsulated extract before digestion showed a first mass loss of about 20% between 0 and 200 °C, followed by a 40% loss between 200 and 410 °C, with a final residual mass of 20% (Fig. 5A). After digestion, the encapsulated extract presented an initial mass loss of 30% up to approximately 125 °C, followed by an additional 30% loss between 125 and 400 °C, retaining 18% of its total mass. Pure PVP exhibited the fastest initial degradation, leaving no residual mass at the end of the analysis. Incorporation of ora-pro-nobis extract, however, improved the thermal stability of PVP by approximately 22%. Mendes et al. [41] observed that incorporating ora-pro-nobis mucilage into PLA/PEG membranes delayed the onset of degradation and improved thermal stability.

The free extract before digestion showed a slight mass loss (5%) in the first degradation phase up to 110 °C. The second stage, from 110 to 500 °C, resulted in a 60% mass loss, while the final stage continued until 600 °C, leaving an 18% residue. After digestion, the free extract showed an initial 10% loss up to 120 °C, followed by a 35% loss up to 300 °C, with a final residue of 38%. Similar patterns were reported by Silva et al. [43] for ora-pro-nobis green fruit mucilage, which presented three degradation stages and retained 39% of its mass at the end of analysis. In contrast, Amaral et al. [54] found almost complete mass loss for ora-pro-nobis leaf mucilage at 600 °C. Oliveira et al. [39] also reported that both pure leaf mucilage and films containing it exhibited residual masses of 28–30% after thermogravimetric analysis.

Both free and encapsulated extracts displayed endothermic peaks between 100 and 150 °C after *in vitro* digestion (Fig. 5C). All samples exhibited three degradation stages, except PVP, which showed only two. The first stage is attributed to water and volatile compound vaporization. The second stage likely corresponds to the onset of biopolymer degradation, including conformational changes, branching cleavage, and polysaccharide and protein breakdown. The final stage is associated with oxidative degradation of carbon and the decomposition of mineral residues [55].

Evaluation of Cytotoxicity

The results of the antiproliferative capacity are presented in Table 3. The free extract and the encapsulated extract were tested against four tumor cell lines and a non-tumor primary culture (PLP2). The results are expressed in GI_{50} values (50% Cell proliferation Inhibition).

The toxicity of the encapsulated extract and the free extract was tested up to a concentration of 400 µg/mL, which is considered the limit for toxicity [51]. Both extracts showed no toxicity to the healthy cells tested (PLP2), with the GI_{50} value being higher than the concentration tested (400 µg/mL). Garcia et al. [17] reported the non-toxicity of

Table 3 Cytotoxicity (IG_{50} values, µg/mL) of the free extract and the encapsulated extract of *P. aculeata* (mean ± SD)

Antiproliferative activity (GI_{50}, µg/mL.)	Free extract	Encapsulated extract
AGS (gastric adenocarcinoma)	>400	299 ± 18
Caco-2 (colorrectal adenocarcinoma)	>400	>400
NCl-H460 (lung carcinoma)	>400	346 ± 28
MCF-7 (breast adenocarcinoma)	>400	>400
PLP2 (porcine liver primary cells)	>400	>400

Results are presented as mean ± standard deviation. GI_{50} values correspond to the extract concentration that causes 50% of cell growth inhibition

Table 4 Mitotic index and index of cellular changes in meristems of *A. cepa* root bulbs exposed for 120 h to PVP, encapsulated extract and free ora-pro-nobis extract

TR	MI/SD	ICC/SD
Co	100 ± 0.8	100 ± 0.5
Encapsulated extract	75.7 ± 0.9	0.5 ± 0.4*
Free extract	80.9 ± 0.8	0.1 ± 0.5*
PVP	95.2 ± 0.7	0.1 ± 0.7*

TR: Treatment; MI: mitotic index; ICC: index of cellular changes, index; SD: standard Deviation; co: control (distilled water). *Significant differences between concentrations and their respective controls, according to Kruskal-Wallis H followed by dunn's post hoc test ($p \leq 0.05$)

ora-pro-nobis leaves against liver cells in culture (PLP2). Mendes et al. [41] evaluated the cytotoxicity of membranes composed of polylactic acid/polyethylene glycol and ora-pro-nobis extract using murine fibroblasts derived from connective tissue (L929) and reported no toxicity.

The encapsulated formulation showed antiproliferative effects against AGS and NCI-H460 cells. Given the multicomponent nature of the formulation (extract + PVP + Tween 80), these findings should be interpreted as exploratory and do not allow attribution of activity to a single component without additional controls or fractionation.

Based on the results in Table 4, it can be seen that none of the treatments caused changes in the mitotic index of the meristematic cells of *A. cepa* roots, showing that they were non-cytotoxic. Also, no significant cellular changes were observed in the root meristems, showing absence of genotoxicity.

Polyphenolic Contents and Antioxidant Activity

Table 5 summarizes the total phenolic content (TPC), total flavonoid content (TFC), and antioxidant activities of free and encapsulated ora-pro-nobis extracts before and after simulated gastrointestinal digestion. In undigested samples, the encapsulated extract exhibited significantly higher TPC than the free extract ($p \leq 0.05$), although both showed a similar proportional decrease after digestion ($p \geq 0.05$). This reduction is probably due to interactions between phenolics and food macromolecules (proteins, starch, dietary fiber, and lipids), which limit their bioavailability [48, 49].

Bioaccessibility, calculated from the TPC and TFC retained after digestion, reached 76.95% and 85.03% in the free extract, and 61.37% and 66.10% in the encapsulated extract, respectively. These values align with previous reports for free ora-pro-nobis extracts [19]. Flavonoid instability under pH shifts and enzymatic activity [56, 57], as well as possible flavonoid–protease complex formation [58, 59], probably contributed to these losses.

Table 5 summarizes the main effects caused by *in vitro* Both extracts-maintained antioxidant activity in all assays. In the DPPH assay, digestion significantly reduced activity

Table 5 Total phenolics, flavonoids, and antioxidant activity of free and encapsulated ora-pro-nobis extracts

Parameter	Free extract	Digested free extract	Encapsulated extract	Digested encapsulated extract	Digestion effect (Free)	Digestion effect (Encapsulated)
Total phenolic content (µg GAE/mg extract)	101.25 ± 3.20^{b}	77.88 ± 1.52^{a}	118.78 ± 1.48^{c}	72.99 ± 0.34^{a}	Decreased	Decreased
Bioaccessibility – phenolics (%)	-	76.92 ± 2.86	-	61.45 ± 0.82	-	-
Total flavonoid content (µg CE/mg extract)	27.87 ± 0.55^{c}	23.70 ± 0.75^{b}	29.47 ± 0.58^{c}	19.48 ± 1.30^{a}	Decreased	Decreased
Bioaccessibility – flavonoids (%)	-	85.04 ± 3.17	-	66.10 ± 4.60	-	-
ABTS (IC_{50} µg·mL^{-1})	60.35 ± 2.70^{a}	72.19 ± 5.54^{b}	54.25 ± 8.98^{a}	62.00 ± 5.41^{ab}	Decreased	No significant change
DPPH (IC_{50} µg·mL^{-1})	52.56 ± 5.38^{a}	68.23 ± 9.76^{b}	51.32 ± 2.59^{a}	64.56 ± 3.17^{ab}	Decreased significantly	No significant change
TBARS (IC_{50} µg·mL^{-1})	35.26 ± 8.13^{a}	292.40 ± 38.18^{c}	143.36 ± 5.06^{b}	719.85 ± 13.08^{d}	−8.29%	−5.02%
FRAP (µmol TE/g extract)	349.46 ± 13.85^{b}	265.35 ± 4.64^{a}	393.75 ± 11.09^{c}	300.83 ± 27.93^{a}	Decreased	Decreased

The means of the samples ($n = 3$) followed by the same super script letter in the same row do not differ significantly from each other ($p > 0.05$). µgGAE/mg extract: micrograms of gallic acid equivalents per milligram of extract. µgCE/mg extract: micrograms of catechin equivalents per milligram of extract. IC_{50} expressed in µg.mL^{-1}. IC_{50}: Extract concentration capable of decolorizing 50% of the evaluated activity. µmolTE/g extract: micromoles of Trolox equivalent per gram of extract. The values of the encapsulated materials were normalized in relation to the values of the non-encapsulated materials

in the free extract but not in the encapsulated form. ABTS radical scavenging, evaluated here for the first time in ora-pro-nobis during *in vitro* digestion, remained stable in encapsulated samples, indicating high encapsulation efficiency. Literature reports show large IC_{50} variations for free extracts in ABTS (40.5–1209.8 µg/mL) and DPPH (72.9–1612.9 µg/mL) assays [8, 17]. In lipid peroxidation assays, digestion reduced activity in both forms, though the decline was smaller for the encapsulated extract (5.02%) than for the free extract (8.29%). These findings agree with previous evidence that bile acid–iron interactions promote lipid peroxidation during digestion [60, 61]. In the FRAP assay, the encapsulated extract was more effective than the free extract before digestion, but digestion decreased ferric-reducing capacity in both cases.

Overall, simulated digestion reduced TPC, TFC, and antioxidant capacity, yet encapsulation preserved activity against ABTS and DPPH radicals. This protective effect probably results from microencapsulation shielding bioactives from pH variation, enzymatic degradation, and oxidation [61]. Consistent with previous reports [19], digestion markedly reduced or eliminated several phenolic acids in ora-pro-nobis extract, including caffeic, fumaric, quinic, citric, malic, and tartaric acids.

Conclusion

The present study demonstrates, for the first time, that the simultaneous extraction and encapsulation of *Pereskia aculeata* leaf extracts in polyvinylpyrrolidone effectively protect phenolic compounds, flavonoids, and antioxidant activity against degradation during simulated gastrointestinal digestion. Compared to free extracts, encapsulated extracts exhibited significantly higher stability and bioaccessibility, highlighting the potential of this approach for preserving functional properties in food and nutraceutical applications. These findings reinforce the value of encapsulation technologies as a strategy to enhance the delivery and efficacy of bioactive compounds from wild food plants such as ora-pro-nobis.

Acknowledgements The authors are indebted to Dr. Adelar Bracht for his style and language corrections and for his technical suggestions for improving description and interpretation.

Author Contributions Valéria Maria Costa Teixeira: Investigation, Formal analysis, Conceptualization, Writing - Original Draft, Software. Anielle de Oliveira: Investigation, Formal analysis. José Rivaldo dos Santos Filho: Investigation, Formal analysis, Writing - Original Draft. Amarilis Santos de Carvalho: Formal analysis. Ashley Uchoa: Formal analysis. Ana Paula Peron: Formal analysis. Filipa Mandim: Formal analysis. Eliana Pereira: Formal analysis. Fernanda Vitoria Leimann: Investigation, Original Draft Writing - Review & Editing, Supervision. Alex Graça Contato: Original Draft Writing - Review & Editing. Rosane Marina Peralta: Investigation, Original Draft Writing - Review & Editing, Supervision.

Funding The Article Processing Charge (APC) for the publication of this research was funded by the Coordenação de Aperfeiçoamento de Pessoal de Nível Superior - Brasil (CAPES) (ROR identifier: 00x0ma614). Valéria Maria Costa Teixeira was a grant recipient of the Coordenação de Aperfeiçoamento de Pessoal de Nível Superior (CAPES). This work was supported by national funds through FCT/MCTES (PID-DAC): CIMO, UIDB/00690/2020 (DOI: https://doi.org/10.54499/UIDB/00690/2020) and UIDP/00690/2020 (DOI: https://doi.org/10.54499/UIDP/00690/2020) and SusTEC, LA/P/0007/2020 (DOI: https://doi.org/10.54499/LA/P/0007/2020).

Data Availability Data will be made available on request.

Declarations

Competing interests The authors declare no competing interests.

References

1. N.C.C. Pinto, M.S.F. Maciel, N.S. Rezende, A.P.N. Duque, R.F.M. Mendes, J.B. da Silva, M.R. Evangelista, L.C. Monteiro, J.M. da Silva, J.C.C. Costa, E. Scio, J. Pharm. Pharmacol. **72**, 1933–1945 (2020)
2. L. Rosa, C.R.A.A. Queiroz, C.M.T. Melo, Biosci. J. **36**, 376–382 (2020)
3. D.O. Silva, M. Seifert, F.R. Nora, V.L. Bobrowski, R.A. Freitag, H.R. Kucera, N.W. Gaikwad, J. Med. Food **20**, 403–409 (2017)
4. M.F. Frankelin, T.F. Vieira, J.A.A. Garcia, R.C.G. Correa, A.R.G. Monteiro, A. Bracht, R.M. Peralta, Phytochemical, nutritional and pharmacological properties of unconventional native fruits and vegetables from Brazil, in *Phytochemicals in Vegetables*. ed. by S.A. Petropoulos, I.C.F.R. Ferreira, L. Barros (Bentham e-books, 2018), pp.444–472
5. S. Mazon, D. Menin, B.M. Cella, C.C. Lise, T.D.O. Vargas, M.L.M. Daltoé, Food Sci. Technol. **40**, 215–221 (2020)
6. L.F. Souza, L. Caputo, I.B.D. de Barros, F. Fratianni, F. Nazzaro, V. de Feo, Int. J. Mol. Sci. **17**, 9 (2016)
7. B.V. Neves, L.M.S. Mesquita, D.C. Murador, A.I.P. Cheberle, A.R.C. Braga, A.Z. Mercadante, V.V. de Rosso, ACS Food Sci. Technol. **7**, 1 (2021)
8. A.M. Massocatto, N.F.S. Silva, C.C. Kazama, M.D.B. Pires, O.S. Takemura, E. Jacomassi, A.L.T.G. Ruiz, A. Laverde Junior, Pharm. Sci. **28**, 156–165 (2022)
9. T.C.L. de Souza, T.F.F. da Silveira, M.I. Rodrigues, A.L.T.G. Ruiz, D.A. Neves, M.C.T. Duarte, E.C.E. Cunha-Santos, G.

Kuhnle, A.B. Ribeiro, H.T. Godoy, Food Chem. **364**, 130350 (2021)
10. A.A. Martin, R.A. de Freitas, G.L. Sassaki, P.H.L. Evangelista, M.R. Sierakowski, Food Hydrocolloids **70**, 20–28 (2017)
11. J.D.M. Macoris, T. Brugnari, C.G. Boer, A.G. Contato, R.M. Peralta, C.G.M. de Souza, Int. J. Curr. Microbiol. Appl. Sci. **6**, 3757–3767 (2017)
12. A.G. Contato, G.M. Aranha, B.A. de Abreu Filho, R.M. Peralta, C.G.M. de Souza, Int. J. Med. Mushrooms. **23**, 1–7 (2021)
13. G.M. Aranha, A.G. Contato, J.C.S. Salgado, T.B. de Oliveira, K.M. Retamiro, G.G. Ortolan, E.J. Crevelin, C.V. Nakamura, L.A.B. de Moraes, R.M. Peralta, M.L.T.M. Polizeli, Braz J. Microbiol. **53**, 349–358 (2022)
14. A.G. Contato, C.A. Conte-Junior, Nutrients. **17**, 1307 (2025)
15. L.F. Ballesteros, M.J. Ramirez, C.E. Orrego, J.A. Teixeira, S.I. Mussatto, Food Chem. **237**, 623–631 (2017)
16. N.C.C. Pinto, D.C. Machado, J.M. Silva, J.L.M. Conegundes, A.C.M. Gualberto, J. Gameiro, L.M. Chedier, M.C.M.N. Castañon, E. Scio, J. Ethnopharmacol. **173**, 330–337 (2015)
17. J.A.A. Garcia, R.C.G. Corrêa, L. Barros, C. Pereira, R.M.V. Abreu, M.J. Alves, R.C. Calhelha, A. Bracht, R.M. Peralta, I.C.F.R. Ferreira, Food Chem. **294**, 302–308 (2019)
18. T.M. Cruz, J.S. Santos, M.A.V. do Carmo, J. Hellström, J.M. Pihlava, L. Azevedo, D. Granato, M.B. Marques, Food Chem. **361**, 130078 (2021)
19. T.M. Cruz, A.S. Lima, F. Zhou, L. Zhang, L. Azevedo, M.B. Marques, D. Granato, Food Chem. **460**, 140484 (2024)
20. D. Chauhan, P.R. Solanki, ACS Appl. Polym. Mater. **1**, 1613–1623 (2019)
21. T. Munir, A. Mahmood, M. Imran, A. Sohail, M. Fakhar-E-Alam, M. Sharif, M. Masood, S.Z. Bajwa, F. Shafiq, Phys. B: Condens. Matter. **602**, 412564 (2021)
22. F. Han, M. Cao, J. Lin, T. Liu, X. Zhu, Y. Zhang, Colloid Polym. Sci. **302**, 355–362 (2024)
23. A. Rehman, S. Yaqub, M. Ali, H. Nazir, N. Shahzad, S. Shakir, J. Mol. Liq. **391**, 123350 (2023)
24. F. Rocha, L.Y. Sugahara, F.V. Leimann, S.M. de Oliveira, E.S. Brum, R.C. Calhelha, M.F. Barreiro, I.C.F.R. Ferreira, R.P. Ineu, O.H. Gonçalves, Food Funct. **9**, 3698–3706 (2018)
25. P.D.F. Santos, C.R.L. Francisco, A. Coqueiro, F.V. Leimann, J. Pinela, R.C. Calhelha, R.P. Ineu, I.C.F.R. Ferreira, E. Bona, O.H. Gonçalves, Food Funct. **10**, 573–582 (2019)
26. J.T.P. Silva, J.M.T. Geiss, S.M. Oliveira, E.D.S. Brum, S.C. Sagae, D. Becker, F.V. Leimann, R.P. Ineu, G.P. Guerra, O.H. Gonçalves, Mater. Sci. Eng. C **76**, 1005–1011 (2017)
27. C.H.K. Santos, M.R. Baqueta, A. Coqueiro, M.I. Dias, L. Barros, M.F. Barreiro, I.C.F.R. Ferreira, O.H. Gonçalves, E. Bona, M.V. da Silva, F.V. Leimann, Food Chem. **261**, 216–223 (2018)
28. L. Barros, E. Pereira, R.C. Calhelha, M. Dueñas, A.M. Carvalho, C. Santos-Buelga, I.C.F.R. Ferreira, J. Funct. Foods **5**, 1732–1740 (2013)
29. F. Mandim, V.C. Graça, R.C. Calhelha, I.L.F. Machado, L.F.V. Ferreira, I.C.F.R. Ferreira, P.F. Santos, Molecules. **24**, 863 (2019)
30. G. Fiskesjö, Hereditas. **102**, 99–112 (1985)
31. A.C.K. Filipi, G.C.S.G. Nascimento, P.A. Bressani, A.K.G. Oliveira, D.E. Santo, C.C.S. Duarte, A.P. Peron, Water Air Soil. Pollut. **234**, 296 (2023)
32. A. Brodkorb, E. Egger, M. Alminger, P. Alvito, R. Assunção, S. Ballance, T. Bohn, C. Bourlieu-Lacanal, R. Boutrou, F. Carrière, A. Clemente, M. Corredig, D. Dupont, C. Dufour, C. Edwards, M. Golding, A.S. Karakay, B. Kirkhus, S. Le Feunteun, I. Recio, Nat. Protoc. **14**, 991–1014 (2019)
33. V.L. Singleton, J. Rossi, Am. J. Enol. Vitic. **16**, 144–158 (1965)
34. M. Alothman, R. Bhat, A.A. Karim, Food Chem. **115**, 785–788 (2009)
35. K. Thaipong, U. Boonprakob, K. Crosby, L. Cisneros-Zevallos, D.H. Byrne, J. Food Compos. Anal. **19**, 669–675 (2006)
36. R.C.G. Corrêa, A.H.P. de Souza, R.C. Calhelha, L. Barros, J. Glamoclija, M. Sokovic, R.M. Peralta, A. Bracht, I.C.F.R. Ferreira, Food Funct. **6**, 2155–2164 (2015)
37. F.S. Reis, A. Martins, L. Barros, I.C.F.R. Ferreira, Food Chem. Toxicol. **50**, 1201–1207 (2012)
38. A.G. Contato, T. Brugnari, A.P.A. Sibin, A.J.R. Buzzo, A.B. de Sá-Nakanishi, L. Bracht, C.A. Bersani-Amado, R.M. Peralta, C.G.M. de Souza, Cell. Biochem. Biophys. **78**, 111–119 (2020)
39. J.L. de Oliveira, Use of the leaf and leaf-extracted material of *ora-pro-nobis* (*Pereskia aculeata* Miller) for the removal of Cd^{2+} and Pb^{2+} ions from aqueous solutions. 2019. 95 pages. Dissertation (Master's in Chemistry) – Federal University of Ouro Preto, Ouro Preto, 2019
40. M. Hadidi, J.C. Orellana-Palacios, F. Aghababaei, D.J. Gonzalez-Serrano, A. Moreno, J.M. Lorenzo, LWT. **169**, 114003 (2022)
41. J.F. Mendes, M.L. Fontes, T.V. Barbosa, R.T. Paschoalin, L.H.C. Mattoso, Int. J. Biol. Macromol. **268**, 131365 (2024)
42. M.C. Conceição, Optimization of the Extraction Process and Characterization of the Mucilage from *Ora-pro-nobis* (*Pereskia aculeata* Miller). 2013. 122 pages. Thesis (Postgraduate Program in Food Science) – Federal University of Lavras, Lavras, 2013
43. S.H. Silva, I.C.O. Neves, N.L. Oliveira, A.C.F. de Oliveira, A.M.T. Lago, T.M.D.O. Giarola, J.V. de Resende, Ind. Crop Prod. **140**, 111716 (2019)
44. M.C.C. Macedo, V.D.M. Silva, M.S.M. Serafim, V.T.C. Correia, D.T.V. Pereira, P.R. Amante, A.S.J. da Silva, H.O.P. Mendonça, R. Augusti, A.C.C.F.F. de Paula, J.O.F. Melo, C.V. Pires, C.A. Fante, Metabolites. **13**, 691 (2023)
45. R.N. Oliveira, M.C. Mancini, F.C.S. de Oliveira, T.M. Passos, B. Quilty, R.M.D.S.M. Thiré, G.B. Mcguinness, Materia. **21**, 167–779 (2016)
46. L.C. de Morais, I.A.F. Ferreira, A.C.F. de Meira, L.A.A. Veríssimo, J.V. de Resende, J. Appl. Polym. Sci. **140**, 2 (2023)
47. E. Bramanti, L. Bonaccorsi, B. Campanella, C. Ferrari, A. Malara, A. Freni, Mater. Chem. Phys. **287**, 126248 (2022)
48. M. Peanparkdee, C. Borompichaichartkul, S. Iwamoto, Food Chem. **361**, 130161 (2021)
49. J. Gao, Y. Mao, C. Xiang, M. Cao, G. Ren, K. Wang, X. Ma, D. Wu, H. Xie, Food Chem. **354**, 129516 (2021)
50. A. Kumar, C.K. Dixit, Methods for characterization of nanoparticles, in *Advances in Nanomedicine for the Delivery of Therapeutic Nucleic Acids*. ed. by S. Nimesh, A. Chandra, N. Gupta (Woodhead Publishing, 2017), pp.43–58
51. K.M. dos Santos, R.M. Barbosa, L. Meirelles, F.G.A. Vargas, A.C.S. Lins, C.A. Camara, C.F.S. Aragão, T.F.L. Moura, F.N. Raffin, J. Therm. Anal. Calorim. **146**, 2523–2532 (2021)
52. I. Biran, L. Houben, A. Kossoy, B. Rybtchinski, J. Phys. Chem. C. (2024). https://doi.org/10.1021/acs.jpcc.3c06977
53. A. de Oliveira, T.F. Moreira, B.P. Silva, G. Oliveira, V.M.C. Teixeira, L.S. Watanabe, S.L. Nixdorf, L.E. Leal, L.G.A. Pessoa, F.A.V. Seixas, O.H. Gonçalves, A.P. Peron, A.B. de Sá-Nakanishi, F.V. Leimann, A. Bracht, J.F. Comar, Food Res. Int. **178**, 113878 (2024)
54. T.N. Amaral, L.A. Junqueira, M.E.T. Prado, M.A. Cirillo, L.R. de Abreu, F.F. Costa, J.V. de Resende, Food Hydrocol. **79**, 331–342 (2018)
55. D. Stojković, M.I. Dias, D. Drakulić, L. Barros, M. Stevanović, I.C.F.R. Ferreira, M.D. Soković, Pharmaceuticals. **13**, 78 (2020)
56. R . Caparica, M. Lambertini, E. de Azambuja, Esmo Open. **4**, e00050 (2019)
57. G. Swiderski, E. Gołębiewska, M. Kalinowska, R. Swisłocka, N. Kowalczyk, A. Jabłońska-Trypuć, W. Lewandowski, Materials. **17**, 2575 (2024)

58. Y. Qin, L. Wang, Y. Liu, Q. Zhang, Y. Li, Z. Wu, J. Funct. Foods **46**, 57–65 (2018)
59. G . Zheng, J. Deng, L. Wen, L. You, Z. Zhao, L. Zhou, J. Funct. Foods **40**, 76–85 (2018)
60. L. Sęczyk, D. Sugier, M. Świeca, U. Gawlik-Dziki, Food Chem. **344**, 128581 (2021)
61. C. Dima, E. Assadpour, S. Dima, S.M. Jafari, Compr. Rev. Food Sci. Food Saf. **19**, 1541–4337 (2020)